Published in final edited form as:

Oncogene. 2014 August 14; 33(33): 4203–4212. doi:10.1038/onc.2013.377.

Macrophage contact induces RhoA GTPase signaling to trigger tumor cell intravasation

Minna Roh-Johnson[1], **J. Javier Bravo-Cordero**[1], **Antonia Patsialou**[1], **Ved P. Sharma**[1], **Peng Guo**[1], **Huiping Liu**[2], **Louis Hodgson**[1], and **John Condeelis**[1]

[1]Department of Anatomy and Structural Biology, Albert Einstein College of Medicine, Bronx, NY, USA, Gruss-Lipper Biophotonics Center

[2]The Ben May Department for Cancer Research, University of Chicago, Chicago, IL, USA

Abstract

Most cancer patients die as a result of metastasis, thus it is important to understand the molecular mechanisms of dissemination, including intra- and extravasation. Although the mechanisms of extravasation have been vastly studied in vitro and in vivo, the process of intravasation is still unclear. Furthermore, how cells in the tumor microenvironment facilitate tumor cell intravasation is still unknown. Using high-resolution imaging, we found that macrophages enhance tumor cell intravasation upon physical contact. Macrophage and tumor cell contact induce RhoA activity in tumor cells, triggering the formation of actin-rich degradative protrusions called invadopodia, enabling tumor cells to degrade and break through matrix barriers during tumor cell transendothelial migration. Interestingly, we show that macrophage-induced invadopodium formation and tumor cell intravasation also occur in patient-derived tumor cells and in vivo models, revealing a conserved mechanism of tumor cell intravasation. Our results illustrate a novel heterotypic cell contact mediated signaling role for RhoA, as well as yield mechanistic insight into the ability of cells within the tumor microenvironment to facilitate steps of the metastatic cascade.

Keywords

cancer; tumor cell intravasation; macrophages; RhoA biosensor; invadopodia; heterotypic cell contact

Corresponding author: minna.roh@einstein.yu.edu, 718-678-1132.

The authors have no conflicts of interests to declare.

Author Contributions:

MR-J and JC conceived the project idea. MR-J, JJB-C, and LH performed RhoA biosensor experiments, LH cloned RhoA mutant constructs, AP maintained TN1-GFP cells, created the MDA-MB-231 dtomato cell line, and performed qRT-PCR; VPS optimized protocols regarding invadopodia assays and helped with microscopy; PG and MR-J performed IMARIS 3D reconstructions, and HL created the TN1-GFP cells. MR-J performed the rest of the experiments. All authors contributed to discussions related to the manuscript. MR-J and JC wrote the manuscript.

Supplementary Information accompanies the paper on the Oncogene website (http://www.nature.com/onc).

Introduction

More than 1 in 3 people will develop cancer in their lifetime, and approximately 1,500 people die from cancer each day in the United States. Understanding the mechanistic basis of specific steps of metastasis is critical for the identification of robust early prognostic markers.

Understanding how tumor cells escape the primary tumor and enter the vasculature (a process termed intravasation) is a key step in designing treatment strategies of the disease. Multiphoton-based intravital imaging of rodent mammary adenocarcinoma (1) and human tumors (Patsialou et al, in prep) have revealed that tumor cells and macrophages cooperate during several key steps of the metastatic cascade. The polarization and subsequent motility of invasive tumor cells toward the blood vessels is dependent on a paracrine loop of signaling with macrophages (2, 3). Tumor cells respond to macrophage-secreted epidermal growth factor (EGF), and in turn, macrophages respond to tumor cell-secreted colony-stimulating factor-1 (CSF-1). Macrophages have also been shown to play a role in tumor cell entry into the vasculature in vitro and in vivo as treatment with drugs that affect macrophage function results in a decreased number of circulating tumor cells (1). However, as both the tumor cells ability to migrate toward the blood vessel as well as the actual intravasation step are both necessary for entry of tumor cells into the circulation, it is still unclear how macrophages affect tumor cell intravasation specifically. Furthermore, recent in vitro studies examining the mechanism of tumor cell intravasation has shown that the presence of macrophages increases tumor cell intravasation, but the mechanisms of this enhancement are still unclear (1, 4).

Intravital imaging of the tumor microenvironment has shown that tumor cells intravasate into the vasculature at sites near macrophages (2). Due to these visualizations, a microanatomic landmark composed of a perivascular macrophage in contact with a tumor cell at blood vessels had been identified and termed TMEM, or Tumor MicroEnvironment of Metastasis. In a case-controlled study of metastastic and nonmetastatic breast cancers, TMEM density in breast tumors at initial resection was associated with risk of metastasis (5), suggesting that macrophages, tumor cells and endothelial cells cooperate for tumor cell entry into the vasculature. However, little is known about the cell biological mechanisms that exist between these three cell types during intravasation.

To gain a closer look at the molecular mechanisms of tumor cell transendothelial migration, in vitro experiments focused on studying tumor cell and endothelial cell behavior have been widely studied. Often, models of tumor cell extravasation, or exit of tumor cells from the vasculature, are used since the apical surface of the endothelial can be easily accessed by plating endothelial monolayers and seeding tumor cells on these monolayers (6–10). From these studies, an extensive view of how tumor cells affect the endothelial cell architecture has been elucidated, and the specific steps of tumor cell adhesion and intercalation during transmigration have been described (6, 7, 11, 12). A common downstream mechanism of tumor cell transendothelial migration is the opening of the endothelial monolayer. Endothelial cells lose their adherens junctions and tight junctions as gaps open in the monolayer, allowing for tumor cell passage. Molecular pathways leading to adhesion

dissolution have also been identified (11, 13, 14). What is less clear, however, is how tumor cells undergo intravasation, and whether common mechanisms exist between intravasation and extravasation. Given that tumor cells withstand shear flow stresses in the blood vessels and that different cells are present at sites of intravasation and extravasation, we predict that different modes of cell-cell interactions occur when tumor cells intravasate versus extravasate. As such, given that macrophages are visualized at sites of tumor cell intravasation in vivo, we sought to explore the link between the close association of macrophages and tumor cells, and the subsequent tumor cell intravasation.

Using dissolution of endothelial cell-cell adhesion as a readout of tumor cell transendothelial migration, we dissected the relationship between macrophages and tumor cells with an in vitro model of intravasation. In particular, we asked if the association of macrophages and tumor cells reflected a cell biological mechanism that supports intravasation. Using high resolution imaging, combined with in vitro and in vivo models, we tested whether macrophages enhance tumor cell intravasation and the cell biological and signaling mechanisms that regulate this process. Our results reveal that macrophages facilitate tumor cell intravasation by inducing the activation of the RhoA signaling pathway resulting in the formation of invadopodia, enabling the tumor cells to initiate intravasation by penetrating through the basement membrane of the vasculature.

Results

Validation of in vitro intravasation assay

To specifically examine the interactions between tumor cells, macrophages and endothelial cells during tumor cell intravasation, we developed an in vitro model to mimic the appropriate endothelial monolayer polarity. Using primary human microvascular endothelial cells (HUVECs), we formed “upside down” endothelial monolayers using transwells for support (Figure 1A). The endothelium was intact, impermeable to large molecules, and displayed high transendothelial electrical resistance (Figure S1A, B). To image the transwells, transwells were placed in glass-bottom dishes and imaged en face at the level of the endothelium (Figure 1A, Figure S1C). We assessed monolayer polarity by immunostaining the endothelium with polarity markers, apical ZO-1 and basal collagen IV, and found that proper polarity was established, with the basal side of the endothelium facing the transwell and the apical side of the endothelium facing the bottom chamber (Figure S1C–F).

Macrophage enhance tumor cell intravasation in vitro

To examine the interactions between tumor cells, macrophages and the endothelium during intravasation, we added a highly metastatic triple negative human breast cancer cell line, MDA-MB-231, and the BAC1.2F5 murine macrophage cell line to the transwells and analyzed the interactions with fixed and live imaging (Figure 1). We have previously shown that the interactions between these cells are not hindered due to species difference (15, 16). With fixed imaging of en face views of the transwells, we found that tumor cells and macrophages made close interactions with each other at the level of the endothelium (Figure 1B). Live imaging of tumor cell transmigration in the transwells revealed that tumor cells

preferentially underwent transendothelial migration at sites where macrophages were present (Figure 1C, D; Movie S1). Tumor cells took approximately 2–3 hours to undergo transendothelial migration (Figure 1C), consistent with published in vivo and in vitro studies indicating that tumor transmigration occurs on the order of several hours (4, 17–20) in contrast to neutrophil migration which occurs on a faster time scale (21).

To determine whether macrophages facilitated tumor cell intravasation in our assay, we compared tumor cell transmigration in transwells in which macrophages were present or absent. Tumor cells exhibited a basal level of intravasation independently of macrophages, however tumor cells exhibited a 3-fold increase in intravasation in the presence of macrophages (Figure 2A–C). We tested several macrophage to tumor cell ratios in our assay and determined that a four-fold increase in macrophages to tumor cell ratio elicited a robust tumor cell intravasation response (Figure S2A). As the BAC1.2F5 macrophage cell line was used for these experiments, we also tested for the ability of other macrophage cell lines to enhance tumor cell intravasation. Using an immortalized bone marrow-derived macrophage cell line (iBMM) (22) as well as the RAW264.7 macrophage cell line, we found that tumor cell transendothelial migration was enhanced (Figure S2B), suggesting that this phenomenon was due to a general mechanism by macrophages and not specific to a particular macrophage cell line. As BAC1.2F5 macrophages generated the most consistent and robust macrophage-induced response, this cell line was used for the remainder of the study.

Although tumor cells exhibited a basal level of intravasation independently of macrophages (Figure 2A, C), we specifically were interested in how macrophages affected tumor cell transmigration since there was a strong correlation between TMEM formation and distant metastases in patients (5). Therefore, we focused our studies on macrophage-induced transendothelial migration. To determine the effects of tumor cell transendothelial migration on endothelial cell-cell adhesion, we examined cell adhesion in transwells during tumor cell crossing. Using multiphoton-based intravital imaging, tumor cell protrusions aligned along endothelial cell-cell contacts in vivo, suggesting that these protrusive structures were probing the endothelial cell adhesions (Figure S3). Indeed tumor cells have been shown to insert into endothelial monolayers between endothelial cells in in vitro models (6). Consistent with these in vivo results, in our in vitro intravasation assay, endothelial cells lost cell-cell adhesion in regions of tumor cell intravasation (Figure 2D), suggesting that tumor cells were undergoing paracellular migration (between endothelial cells) versus transcellular migration (through endothelial cells) (Figure 2D). This paracellular migration was also reflected in live movies in which tumor cells were visualized to migrate between endothelial cells (Figure 1C). To determine whether the observed paracellular migration was induced by macrophages, we quantified the number of paracellular migration events that occurred when tumor cells were in contact with macrophages versus those that were independent of macrophages. Tumor cells were seen to be in contact with macrophages 86% of the time during paracellular transmigration (Figure 2E), suggesting that the intravasation is a macrophage-induced phenomenon.

Macrophages induce invadopodium formation in tumor cells upon physical contact

From the above results, we determined that the presence of macrophages correlated with tumor cell intravasation; therefore, we next sought to determine the cell biological mechanism by which this induction occurred. We hypothesized that tumor cells must degrade the basal lamina of the endothelium during transmigration. Since breast cancer cell lines were known to form invadopodia, actin-rich structures that degrade matrix, we tested whether macrophages were capable of inducing the formation of invadopodia in breast cancer cells during transendothelial migration, as the formation of invadopodia during this process has been speculated to occur in vivo and in vitro, but never unequivocally shown (23–26). To address this question, we first assayed for the formation of macrophage-induced invadopodia in 2D, and then assayed for the formation of macrophage-induced invadopodia during in vitro intravasation.

In our 2D assay, the formation of invadopodia was detected by subcellular punctate structures formed at the ventral surface of cells that are positive for two invadopodium markers, tks5 and cortactin (27, 28). Tks5 is an adaptor protein necessary for invadopodium formation (29) and cortactin is an actin-binding protein shown to localize and function at invadopodia (27, 28, 30, 31). MDA-MB-231 cell lines have been shown to form invadopodia readily when plated in full serum and/or upon EGF stimulation, even in the absence of macrophages (27, 28, 32, 33). To study the role of macrophages in the formation and function of invadopodia in tumor cells, we first serum-starved the tumor cells and then introduced macrophages. When MDA-MB-231 cells were in serum-starvation conditions, they form few invadopodia, with a majority of the cells forming none at all (control panels; Figure 3A,B). However, when serum-starved MDA-MB-231 cells were cocultured in the presence of macrophages, we found that tumor cells in direct contact with macrophages formed an average of five functional invadopodia, that contained both cortactin and tks5 invadopodium markers and were capable of degrading matrix (Figure 3A,B). These findings were in contrast to the average number of invadopodia formed by tumor cells not in physical contact with macrophages (Figure 3A), which was similar to that of tumor cells that were plated alone (Figure 3B). These experiments suggest that direct physical contact was necessary between the tumor cells and macrophages for macrophage-induced invadopodium formation. To confirm this hypothesis, we performed macrophage conditioned media experiments to stimulate tumor cells. Macrophage conditioned media did not increase the number of invadopodia compared to control media (Figure 3C), further suggesting that physical contact between macrophages and tumor cells was required for enhanced invadopodium formation.

Macrophage-induced invadopodia form and are necessary for tumor cell intravasation

Since the formation of invadopodia was induced by macrophages on 2D matrices, we next tested whether invadopodia could be induced by macrophages during tumor cell intravasation. Tumor cells were first transfected with cortactin-tagRFP to assess the formation of invadopodia. Regions of tumor cell transendothelial migration were detected by a loss of endothelial cell-cell adhesion, as visualized by tight junction immunostaining. Tumor cells indeed accumulated the invadopodium marker, cortactin, in areas of the tumor cell that penetrated through endothelial barriers (Figure 4A, red arrow) forming an invasive

front similar to that previously shown in three dimensional collagen matrices (32, 34), suggesting that invadopodia formed during intravasation. We also found that an independent invadopodium marker, Tks5, is also enriched in areas of the tumor cell that penetrate the endothelium (Figure S4A, green arrow). To determine whether invadopodia are indeed necessary for efficient intravasation, tks5 was knocked down in tumor cells and assessed for their ability to undergo intravasation. Consistent with published results, cells with either transient or stable knockdown of tks5 did not form invadopodia on 2D substrates (29); Figure 4B–E; Figure S4B,C). Transient or stable Tks5 KD cells also did not undergo intravasation even in the presence of macrophages and their level of crossing was similar to background levels (Figure 4F; Figure S4D). Furthermore, treating tumor cells with an MMP inhibitor, GM6001, which has been shown to inhibit the ability of invadopodia to degrade matrix (31), resulted in the inability of tumor cells to cross the endothelium (Figure 4F,G), further suggesting invadopodia are required for intravasation. Given that tks5 KD cells do not exhibit motility defects (29), these experiments strongly suggest that the matrix degrading ability of macrophage-induced invadopodium formation is necessary for tumor cell intravasation.

Patient-derived breast tumor cells form invadopodia and physically contact macrophages during tumor cell intravasation

As the MDA-MB-231 breast cancer cell line is triple negative for the estrogen receptor, progesterone receptor, and human epidermal growth factor receptor 2, we sought to validate our findings with another triple negative receptor cell line. To add clinical relevance to our findings, we used breast tumor cells derived from a patient with triple negative breast cancer, TN1, which are capable of invasion and spontaneous metastasis (35). Since these primary cells do not grow in culture as a cell line, TN1 tumors were grown orthotopically in mice and the tumor cells were dissociated and assayed for their ability to undergo macrophage-dependent transendothelial migration and invadopodium formation in vitro.

We found that TN1 cells exhibited macrophage-induced invadopodium formation (Figure 5A–D; Figure S5). We further found that TN1 cells preferentially underwent intravasation when in contact with macrophages, consistent with our findings with MDA-MB-231 cells (Figure 5E–I). When we quantified the amount of transmigration that occurred, we found that 86% of TN1 cells physically contacted macrophages when undergoing paracellular migration, which was similar to our findings with MDA-MB-231 cells (Figure 5I, compare to Figure 2E). Thus, our experiments with patient-derived breast tumor cells recapitulate our in vitro intravasation results with cell lines.

Physical contact between macrophages and tumor cells correlate with invadopodium formation in vivo

Our in vitro results with both cell lines and patient-derived cells suggest that contact between macrophages and tumor cells induce invadopodium formation in tumor cells to facilitate tumor cell intravasation. To validate these findings in vivo, we generated orthotopic MDA-MB-231 tumors in immune-compromised mice. Once tumors reached 1–1.2cm, the tumors were removed, sectioned and immunostained for blood vessels, macrophages and invadopodia. Specifically, we tested whether tumor cells upregulate

invadopodia markers when in physical contact with macrophages near blood vessels in vivo. We found that this was indeed the case, and tumor cells that were in physical contact with macrophages formed cortactin-rich structures next to blood vessels, compared to cells at the blood vessel that were not in contact with macrophages (Figure 6A,B). These experiments suggest that physical contact between macrophages and tumor cells induce invadopodium formation at blood vessels in vivo.

Macrophages activate RhoA signaling in tumor cells to induce invadopodium formation upon physical contact

We have shown that macrophages induce tumor cell invadopodium formation upon physical contact for intravasation. We next sought to determine the molecular mechanism of this heterotypic cell contact. RhoA, a member of the Rho family of GTPases, was shown to be involved in invadopodium formation (36, 37), and RhoC GTPase has been shown to affect invadopodium morphology and function without affecting invadopodium number (37). As we had visualized changes in invadopodium number upon macrophage contact, we hypothesized that RhoA activity may be induced upon contact with macrophages. Furthermore, RhoA acts as a central node of signaling when cells are mechanically stimulated during processes such as cell-cell interactions (38). Consistent with previous data revealing that knocking down RhoA expression led to reduced matrix degradation (36), we found that knocking down RhoA expression in tumor cells reduced invadopodium formation (Figure S6A,B) and inhibited the ability for macrophages to induce invadopodium formation (Figure S6C). We further found that knocking down RhoA expression resulted in decreased tumor cell intravasation in vitro (Figure S6D). We next tested whether constitutive active mutations of RhoA was sufficient to induce invadopodia in the absence of macrophage contact and found that this was indeed the case, as tumor cells expressing either G14V-RhoA or F30L-RhoA constitutive active mutations formed more invadopodia than WT RhoA in the absence of macrophage contact (Figure S6E).

We next used a RhoA biosensor in tumor cells to monitor the RhoA activation in real time upon physical contact with macrophages. RhoA biosensor expressing cells that did not contact macrophages maintained a constant level of RhoA activity (Figure 7A, C; Figure S7A; Movie S2, S3). However, when macrophages contacted tumor cells (Figure 7B, top DIC panels and inset), there was a global increase in RhoA activity that was sustained for 30 minutes (Figure 7C; Figure S7B; Movie S4, S5). The increase in RhoA activity was concomitant with multiple cell protrusions globally around the tumor cell (Figure 7B, Figure S7B; white arrows), a previously described indicator of increased RhoA activity (39). To determine whether this global increase in RhoA activity led to the formation of invadopodia, we first imaged RhoA biosensor-expressing tumor cells for RhoA activity, and then subsequently assessed the same cells for their ability to form invadopodia upon RhoA activation. We found that tumor cells that were in contact with macrophages and exhibited a global increase in RhoA activity formed significantly more invadopodia than control (Figure 7D, E). Furthermore, these experiments suggest that macrophages induce RhoA GTPase signaling in tumor cells to trigger invadopodium formation for intravasation.

Discussion

While there is a breadth of research exploring how tumor cells affect endothelial cell-cell adhesion, and cytoskeletal mechanisms of extravasation has been vastly studied, little is known about the initial steps of tumor cell intravasation and how other cells within the tumor microenvironment affect this process. Our experiments yield an unexpected finding that macrophages induce RhoA activity and the subsequent enhanced invadopodium formation in breast cancer cells, and that this induction requires physical contact between the two cell types. We have further shown that this macrophage-induced invadopodium formation facilitates tumor cell intravasation using breast cancer cell lines and patient-derived tumor cells, consistent with the hypothesis that invadopodium formation is necessary for tumor cells to degrade the basal lamina overlying blood vessels. These experiments yield mechanistic insight into the formation of TMEM sites in patients that develop distant metastasis. The tripartite structure involving tumor cells, macrophages and endothelial cells found in patients developing distant metastasis may reflect the cell biological mechanism of macrophage-induced invadopodia described in this study.

Invadopodium formation is the first step in tumor cell intravasation

Our results reveal that invadopodia form and are necessary for intravasation. While this phenomenon has been alluded to in the literature, it has never been clearly shown. In vivo studies show that knocking down genes required for invadopodium formation such as N-Wasp, Arg, tks5, or overexpressing proteins resulting in excess invadopodia, result in decreased distant metastasis and/or number of circulating tumor cells (23, 40–42). Several steps are required from primary tumor growth to distant metastasis, so it is difficult to ascertain which specific step of the metastatic cascade is perturbed when tumor cells are unable to form invadopodia. By taking an in vitro approach, we are able to show that invadopodia do indeed form during transendothelial migration, and that invadopodia are also necessary for tumor cell transendothelial migration to occur. Furthermore, we confirm our findings in vivo and show using a blood vessel marker to clearly demarcate where vessels lie in the tumor, tumor cells form invadopodia at sites of intravasation. Interestingly, invadopodia have been suggested to be dispensable for extravasation in vivo (42), revealing a potentially marked difference between mechanisms of intravasation versus extravasation.

Previous experiments suggest that upon tumor cell attachment onto the endothelium, endothelial cells activate Src and other signaling cascades such as p38 and ERK1/2 leading to decreased endothelial cell-cell adhesion, and changes in the endothelial cell actin architecture to facilitate tumor cell crossing (43–49). Whether invadopodia are required to directly disassemble cell-cell adhesion is unknown. However, we hypothesize that the interaction between perivascular macrophages and tumor cells to induce invadopodium formation comprises only the first step in tumor transmigration, and that invadopodium formation is necessary for the tumor cells to penetrate through the basement membrane of the blood vessel to then make contact with the underlying endothelial cells. Subsequent downstream steps requiring loss of endothelial cell-cell adhesion is necessary for completion of tumor cell crossing. Tumor cells also adopt changes in their cytoskeleton to facilitate transmigration (11, 13, 50). Consistent with previous endothelial cell-cell adhesion studies,

we have shown that endothelial cells clearly detach from one another as tumor cells cross through the monolayer, and that tumor cells primarily undergo paracellular transendothelial migration in our in vitro assays.

The role of tumor associated macrophages during tumor cell intravasation

Macrophages are critical players in metastasis, and several macrophage subtypes reside within the tumor microenvironment. We hypothesize that the perivascular macrophages comprise a specific macrophage subtype that facilitates tumor cell intravasation by inducing invadopodium formation in the tumor cell. This does not preclude any other role for macrophages in inducing perturbations in the blood vessels, or signaling that may occur between macrophages and endothelial cells during intravasation. Multiphoton based intravital imaging reveals that while tumor associated macrophages are highly motile, the perivascular macrophages remain stationary, closely docked at blood vessels, and that in some instances, perivascular macrophages can be seen in close association with intravasating tumor cells (3). In this work, we show that macrophages induce RhoA activation and the subsequent formation of invadopodia during transmigration. Certainly, other cell types in the tumor microenvironment also affect tumor cell invadopodium formation and intravasation (Figure S8), revealing the complexity of the tumor microenvironment. Interestingly, only those cell types tested that are capable of inducing invadopodium formation in tumor cells are also capable of enhancing tumor cell intravasation (Figure S8). We predict that invadopodium formation is necessary for several steps of the metastastic cascade, and that there will be different levels of regulation by macrophages and other factors in the tumor microenvironment at each of these steps.

A novel heterotypic cell contact role for RhoA signaling

Recent advances in imaging RhoA activity in vivo reveal subcellular spatial regulation of RhoA activity in cancer models (51, 52). Consistent with these findings, we reveal that macrophages and tumor cells require physical cell-cell contact to induce RhoA activation and subsequent invadopodium formation. GTPases are involved in the formation of homotypic cell-cell contacts in vivo and in vitro, mainly though regulating the integrity of junctions within a sheet of cells (53–57). While RhoA activity has been shown in nascent *homotypic* cell-cell contacts (58), it remained unclear how *heterotypic* cell contacts regulate RhoA activity in real-time. Additionally, although the EGF/CSF-1 paracrine loop of signaling was identified between tumor cells and macrophages, the intracellular signaling pathways induced by macrophages in the tumor microenvironment were elusive. Indeed, the EGF/CSF-1 paracrine loop of signaling is also required for both macrophage-induced invadopodium formation and transendothelial migration (Figure S9). However, as these are known to be secreted molecules, it remains to be determined which upstream contact-mediated signaling between cells in the tumor microenvironment is important for invadopodium formation during transmigration. We hypothesize that the yet unidentified contact mediated ligand-receptor pair will activate the RhoA pathway, resulting in increased invadopodium formation in tumor cells at blood vessels. Our results illustrate a novel role for RhoA in real-time in heterotypic cell-cell contact signaling. The global RhoA increase in the tumor cell, not just at the site of cell contact, suggests that RhoA signaling stimulates invadopodium formation, not merely the location where invadopodia will form. Work

exploring upstream signaling pathways regulating RhoA activity during intravasation is currently underway.

Clinical significance of macrophage-induced intravasation

Using patient-derived breast tumor cells, we confirmed our findings that macrophages induce both invadopodium formation and intravasation in vitro. Broadly, the close association of macrophages and tumor cells at the level of the endothelium lends credence to the finding of TMEM sites in resected tumor tissue of breast cancer patients. Thus, our results support the value of using the number of TMEM sites as a prognostic marker of the risk of distant metastasis.

Methods

Cell lines

MDA-MB-231 and Jurkat T-cells were cultured in 10% FBS/DMEM. MDA-MB-231 cells were serum-starved in 0.5% FBS/0.8% BSA in DMEM for 16 hours prior to macrophage induction studies. BAC1.2F5 cells were cultured in 10% FBS/MEM supplemented with 2mM L-glutamine, 22μg/mL L-asparagine, and 3 000 U/mL of purified human recombinant CSF-1 (generously provided by Richard Stanley, Albert Einstein College of Medicine). Human umbilical vein endothelial cells (HUVECs, Lonza) were cultured in EGM-2 (Lonza) and only used between passage 2–4. Immortalized bone marrow-derived macrophages (22) were cultured in 10% FBS/MEM supplemented with 2 mM L-glutamine, 22 μg/mL L-asparagine, and 10 000 U/mL of purified human recombinant CSF-1. RAWs cells were cultured in 10% FBS/RPMI. HL-60 cells were cultured and differentiated as described (59). TN1 cells were isolated and stably labeled to express GFP as described (35) and maintained by passage through orthotopic injections of mice (Supplementary Materials and Methods).

DNA siRNA and transfection and cell labelling

1×10^6 MDA-MB-231 cells were transfected by 2μg each of Cortactin-tagRFP (27) and GFP-tks5 (kindly provided by Sara Courtneidge), or 1.5μg each of RhoA-WT, RhoA-F30L, RhoA-G14V using the Lonza Nucleofection Kit V protocol 24 hours prior to the experiment using manufacturer conditions. Control nonsilencing siRNA was from Qiagen. Human-specific tks5 and RhoA siGenome Smart Pool were from Dharmacon. 1×10^6 MDA-MB-231 cells were transfected with 2μM siRNA using the Lonza Nucleofection Kit V 72 hours (for tks5) and 96 hours (for RhoA) prior to each experiment. Immunoblot analysis was used to confirm knockdown for each experiment. BAC1.2F5 and HUVECs were labeled with cell tracker dyes (CMFDA, CMPTX from Invitrogen) prior to experiments. Stable cell lines or MDA-MB-231-EGFP and MDA-MB-231-dTomato were made as described (15), with the exception that dTomato was inserted into the EGFP site in the EGFP-C1 vector (Clontech).

Cloning RhoA constitutive active mutants

Expression constructs for the RhoA F30L and G14V mutants were produced and cloned into the pTRIEX-4 backbone (Novagen) as described (Supplementary Materials and Methods).

Inhibitors and blocking antibodies

For in vitro transendothelial migration and invadopodia formation assays, the mouse CSF-1 receptor was blocked with antimouse CSF-1R blocking antibody (AFS98, Novus Biologicals) at a concentration of 5μM, and a Rat IgG1 k isotype control blocking antibody was also used at 5μM. To block the EGF receptor, Iressa (AstraZeneca) was used at 5μM. To block matrix metalloproteases, GM6001 (BML-E1300-0001, Enzo Life Sciences) was used at 5μM.

Western Blotting and quantification

Cells were transfected with tks5, RhoA, or control siRNA for 72 or 96 hours, lysed with SDS-PAGE sample buffer, sonicated and boiled at 95°C. To maintain TN1 cells, tumors of approximately 1 cm in diameter were excised and trimmed, mechanically dissociated with scalpels, and then enzymatically digested for 1 hour at 48°C (Liberase TH, Roche). Samples were filtered twice into a single cell suspension in PBS/2% FBS, red blood cells lysed with ACK buffer (Invitrogen, A10492-01), and cell washed twice with PBS/2% FBS on ice.

RNA extraction and PCR amplication

RNA was extracted from triplicate plates of control and tks5 siRNA 72 hour knockdown plates with RNeasy Mini kit (Qiagen, Valencia, CA, USA). The RNA was evaluated, reverse transcribed and quantitative PCR analysis (Tks5 forward primer 5′-ACCCAAGGACAACAACCTGT-3′; Tks5 reverse primer 5′-AGCGAGCAGTGCTAAAGGAG-3′) was performed as described (42).

Invadopodium assay

405 gelatin-labelled Mattek dishes were made as previously described (60). Tumor cells were plated in complete media for 4 hours on Alexa 405 labelled gelatin dishes. Dishes were fixed and immunostained for cortactin and tks5 as previously described (27). Cells were imaged with a Deltavision Core Microscope (Applied Precision) using a CoolSnap HQ2 camera, 60X 1.42 N.A. oil immersion objective, and softWorx software. Fixed cells were imaged in PBS at room temperature. Invadopodia were detected as punctate structures that were positive for both cortactin and tks5, and capable of degrading Alexa 405-gelatin.

Macrophage-induced invadopodia assay

MDA-MB-231 and TN1-GFP cells were serum starved for 16 hours. BAC1.2F5 cells were cell tracker labeled (CMPTX, Invitrogen). 25K MDA-MB-231 cells were incubated with 125K BAC1.2F5 cells in serum starvation media on 405-labelled gelatin coated dishes for 4 hours, fixed and immunostained for invadopodia markers as described above. For conditioned media experiments, BAC1.2F5 cells were incubated with complete media, with the exception that 300 U/mL CSF-1 was used rather than 3 000 U/mL CSF-1, for 24 hours, and subsequently used for assays. Unconditioned complete media with 300 U/mL CSF-1 was used as a control.

To assess other cell types' ability to induce tumor cell invadopodia, 125K of HL-60 or Jurkat T-cells were incubated with 25K MDA-MB-231 cells in serum starvation media as described above.

In vitro intravasation assay

8-micron pore sized transwell inserts (Millipore) were inverted and the filter was plated with 50uL of 2.5 μg/mL of growth factor reduced matrigel (BD) in DMEM media (Invitrogen) for 1 hour at room temperature. Excess matrigel was removed, and 100K HUVECs were plated on the matrigel-coated filters on the inverted transwells in 50μL EGM-2 for 4 hours in a 37°C CO2 incubator. Transwells were then flipped right side up into a 24 well plate (Corning) and tumor cells and macrophages or other cell types were added as described (Supplementary Materials and Methods). To assess the extent of tumor cell transendothelial migration, transwells were washed twice with PBS and then fixed in 4% paraformaldehyde/PBS for 20 minutes, permeabilized 0.1% triton X-100 for 10 minutes and stained with rhodamine-phalloidin (Invitrogen) and DAPI for 1 hour. Transwells were placed in PBS on a Mattek dish (MatTek Corp) and imaged on an inverted Multiphoton Olympus FV1000-MPE microscope with a 25X NA 1.05 water immersion objective and a Spectra Physics Mai Tai-DeepSee laser set to 880nm. 2μm step Z-stacks of en face views were acquired throughout the depth of the transwell, and only those tumor cells that breached the endothelium were scored as a positive transendothelial migration event. Approximately 6 fields of view were acquired for each transwell.

Transwells were immunostained with ZO-1 (Invitrogen) and Collagen IV (Abcam) antibodies following a previously described protocol (61) and imaged as described (Supplementary Materials and Methods).

To live image the transwells, transwells were set up as described above, and prior to imaging on an inverted Multiphoton Olympus FV1000-MPE microscope with a 25X NA 1.05 water immersion objective and a Spectra Physics Mai Tai-DeepSee laser set to 880nm, the transwells were placed in Mattek dishes with L-15/10% FBS. 2 micron step Z-stacks, encompassing the most apical 10 microns of the transwells were taken every 10 minutes for 3 hours.

Transwell permeability and TEER measurements

Endothelial monolayers were grown on transwells as described above. 1mg/mL 60K texas red dextran was added to the top well. 50uL of media was taken from the bottom well after 30 and 60 minutes, and fluorescence measurements were determined with the described settings for costar 96-well plates, 555/640 using a Fluostar Optima. Transendothelial electrical resistance measurements were made on the same transwells using an EVOM2 epithelial Voltohmmeter (World Precision Instruments).

In vivo imaging and immunostaining

All experiments conducted in mice were in accordance with the National Institutes of Health regulation on the use and care of experimental animals and approved by the Albert Einstein College of Medicine Animal Use Committee. MDA-MB-231 orthotopic tumors were

generated by injected MDA-MB-231 cells expressing GFP in sterile PBS/20% collagen I into the mammary fat pad of severe combined immunodeficiency mice (SCID) mice (NCI, Frederick, MD). Tumors grew for approximately 3 months until they reached 1 cm in size. To image tumor cell interactions with the blood vessel in vivo, mice were injected by tail vein with 50 μL of rhodamine-labelled Ricinus Communis Agglutinin I (Vector Labs). Animals were sacrificed immediately after injection, the tumors were removed and imaged in PBS on an Olympus FV1000-MPE microscope with a 25X NA 1.05 water immersion objective and a Spectra Physics Mai Tai-DeepSee laser set to 880nm. 2um step size Z-stacks were taken for each field of view. For immunostaining of tumor sections, tumors were removed and frozen on dry ice in OCT Compound (TissueTek), sectioned, fixed, immunostained and imaged as described (Supplementary Materials and Methods).

RhoA Biosensor Imaging and Quantification

MDA-MB-231 cells were transiently transfected with the RhoA biosensor (39) using the Lonza Nucleofection protocol described above and plated directly onto MatTek dishes, serum starved overnight, and imaged in a single plane for 3-color imaging every 2 minutes using a previously described protocol (37, 62). Ratiometric calculations on the CFP and YFP FRET emissions of RhoA were performed as described (37, 39). Cells were subsequently fixed and immunostained using methods described above and quantified with the DeltaVision Core microscope using methods described above. For more information, see Supplementary Materials and Methods.

Statistical Analysis

Statistical analysis was conducted using an unpaired, two-tailed Student's T-test when comparing two data sets. Statistical significance was defined as a $p < 0.05$. For multiple comparisons, ANOVA was used. All graphs are displayed as mean ± SEM, unless otherwise indicated. The "n" in SEM was derived from number of fields of view (for tumor cell intravasation) or number of cells (for invadopodium formation).

Supplementary Material

Refer to Web version on PubMed Central for supplementary material.

Acknowledgments

We thank Brian Beaty for advice regarding invadopodia experiments; David Entenberg, Vera Desmarais, Jeffrey Wyckoff, and the Analytical Imaging Facility for help with microscopy; Richard Stanley, Fernando Macian, Esther Arwert, Allison Harney, and Veronika Micolski for guidance and reagents; Yarong Wang for help with animal injections; and the Albert Einstein shRNA Core, the Flow Cytometry Core facility and the Histology and Comparative Pathology Core for help with experiments. We also thank Jeffrey Segall, Dianne Cox, Anne Bresnick and Aviv Bergmann for helpful discussions, and the Condeelis, Segall, Cox and Hodgson labs for advice and reagents. This work was funded by NIH CA150344 (JC), NIH CA100324 (JJB-C and AP), NIH GM093121 (LH), Komen Fellowship KG111405 (VPS), and NIH 1F32CA159663 (MRJ).

References

1. Roussos ET, Balsamo M, Alford SK, Wyckoff JB, Gligorijevic B, Wang Y, et al. Mena invasive (MenaINV) promotes multicellular streaming motility and transendothelial migration in a mouse

model of breast cancer. Journal of cell science. 2011; 124(Pt 13):2120–31. Epub 2011/06/15. [PubMed: 21670198]

2. Wyckoff J, Wang W, Lin EY, Wang Y, Pixley F, Stanley ER, et al. A paracrine loop between tumor cells and macrophages is required for tumor cell migration in mammary tumors. Cancer research. 2004; 64(19):7022–9. Epub 2004/10/07. [PubMed: 15466195]
3. Wyckoff JB, Wang Y, Lin EY, Li JF, Goswami S, Stanley ER, et al. Direct visualization of macrophage-assisted tumor cell intravasation in mammary tumors. Cancer research. 2007; 67(6): 2649–56. Epub 2007/03/17. [PubMed: 17363585]
4. Zervantonakis IK, Hughes-Alford SK, Charest JL, Condeelis JS, Gertler FB, Kamm RD. Three-dimensional microfluidic model for tumor cell intravasation and endothelial barrier function. Proceedings of the National Academy of Sciences of the United States of America. 2012; 109(34): 13515–20. Epub 2012/08/08. [PubMed: 22869695]
5. Robinson BD, Sica GL, Liu YF, Rohan TE, Gertler FB, Condeelis JS, et al. Tumor microenvironment of metastasis in human breast carcinoma: a potential prognostic marker linked to hematogenous dissemination. Clinical cancer research : an official journal of the American Association for Cancer Research. 2009; 15(7):2433–41. Epub 2009/03/26. [PubMed: 19318480]
6. Reymond N, Im JH, Garg R, Vega FM, Borda d'Agua B, Riou P, et al. Cdc42 promotes transendothelial migration of cancer cells through beta1 integrin. The Journal of cell biology. 2012; 199(4):653–68. Epub 2012/11/14. [PubMed: 23148235]
7. Reymond N, Riou P, Ridley AJ. Rho GTPases and cancer cell transendothelial migration. Methods Mol Biol. 2012; 827:123–42. Epub 2011/12/07. [PubMed: 22144272]
8. Jin F, Brockmeier U, Otterbach F, Metzen E. New insight into the SDF-1/CXCR4 axis in a breast carcinoma model: hypoxia-induced endothelial SDF-1 and tumor cell CXCR4 are required for tumor cell intravasation. Molecular cancer research : MCR. 2012; 10(8):1021–31. Epub 2012/07/07. [PubMed: 22767589]
9. Haidari M, Zhang W, Caivano A, Chen Z, Ganjehei L, Mortazavi A, et al. Integrin alpha2beta1 mediates tyrosine phosphorylation of vascular endothelial cadherin induced by invasive breast cancer cells. The Journal of biological chemistry. 2012; 287(39):32981–92. Epub 2012/07/27. [PubMed: 22833667]
10. Haidari M, Zhang W, Chen Z, Ganjehei L, Warier N, Vanderslice P, et al. Myosin light chain phosphorylation facilitates monocyte transendothelial migration by dissociating endothelial adherens junctions. Cardiovascular research. 2011; 92(3):456–65. Epub 2011/09/13. [PubMed: 21908648]
11. Voura EB, Sandig M, Kalnins VI, Siu C. Cell shape changes and cytoskeleton reorganization during transendothelial migration of human melanoma cells. Cell and tissue research. 1998; 293(3):375–87. Epub 1998/08/26. [PubMed: 9716727]
12. Voura EB, Sandig M, Siu CH. Cell-cell interactions during transendothelial migration of tumor cells. Microscopy research and technique. 1998; 43(3):265–75. Epub 1998/12/05. [PubMed: 9840805]
13. Stoletov K, Montel V, Lester RD, Gonias SL, Klemke R. High-resolution imaging of the dynamic tumor cell vascular interface in transparent zebrafish. Proceedings of the National Academy of Sciences of the United States of America. 2007; 104(44):17406–11. Epub 2007/10/24. [PubMed: 17954920]
14. Tremblay PL, Auger FA, Huot J. Regulation of transendothelial migration of colon cancer cells by E-selectin-mediated activation of p38 and ERK MAP kinases. Oncogene. 2006; 25(50):6563–73. Epub 2006/05/23. [PubMed: 16715142]
15. Patsialou A, Wyckoff J, Wang Y, Goswami S, Stanley ER, Condeelis JS. Invasion of human breast cancer cells in vivo requires both paracrine and autocrine loops involving the colony-stimulating factor-1 receptor. Cancer research. 2009; 69(24):9498–506. Epub 2009/11/26. [PubMed: 19934330]
16. Das SK, Stanley ER, Guilbert LJ, Forman LW. Human colony-stimulating factor (CSF-1) radioimmunoassay: resolution of three subclasses of human colony-stimulating factors. Blood. 1981; 58(3):630–41. Epub 1981/09/01. [PubMed: 6973347]

17. Koop S, MacDonald IC, Luzzi K, Schmidt EE, Morris VL, Grattan M, et al. Fate of melanoma cells entering the microcirculation: over 80% survive and extravasate. Cancer research. 1995; 55(12):2520–3. Epub 1995/06/15. [PubMed: 7780961]
18. Kramer RH, Nicolson GL. Interactions of tumor cells with vascular endothelial cell monolayers: a model for metastatic invasion. Proceedings of the National Academy of Sciences of the United States of America. 1979; 76(11):5704–8. Epub 1979/11/01. [PubMed: 293673]
19. Nicolson GL. Metastatic tumor cell attachment and invasion assay utilizing vascular endothelial cell monolayers. The journal of histochemistry and cytochemistry : official journal of the Histochemistry Society. 1982; 30(3):214–20. Epub 1982/03/01. [PubMed: 7061823]
20. Ohigashi H, Shinkai K, Mukai M, Ishikawa O, Imaoka S, Iwanaga T, et al. In vitro invasion of endothelial cell monolayer by rat ascites hepatoma cells. Japanese journal of cancer research : Gann. 1989; 80(9):818–21. Epub 1989/09/01. [PubMed: 2513297]
21. Proebstl D, Voisin MB, Woodfin A, Whiteford J, D'Acquisto F, Jones GE, et al. Pericytes support neutrophil subendothelial cell crawling and breaching of venular walls in vivo. The Journal of experimental medicine. 2012; 209(6):1219–34. Epub 2012/05/23. [PubMed: 22615129]
22. Yu W, Chen J, Xiong Y, Pixley FJ, Dai XM, Yeung YG, et al. CSF-1 receptor structure/function in MacCsf1r−/− macrophages: regulation of proliferation, differentiation, and morphology. Journal of leukocyte biology. 2008; 84(3):852–63. Epub 2008/06/04. [PubMed: 18519746]
23. Gligorijevic B, Wyckoff J, Yamaguchi H, Wang Y, Roussos ET, Condeelis J. N-WASP-mediated invadopodium formation is involved in intravasation and lung metastasis of mammary tumors. Journal of cell science. 2012; 125(Pt 3):724–34. Epub 2012/03/06. [PubMed: 22389406]
24. Yamaguchi H. Pathological roles of invadopodia in cancer invasion and metastasis. European journal of cell biology. 2012; 91(11–12):902–7. Epub 2012/06/05. [PubMed: 22658792]
25. Saltel F, Daubon T, Juin A, Ganuza IE, Veillat V, Genot E. Invadosomes: intriguing structures with promise. European journal of cell biology. 2011; 90(2–3):100–7. Epub 2010/07/08. [PubMed: 20605056]
26. Linder S, Wiesner C, Himmel M. Degrading devices: invadosomes in proteolytic cell invasion. Annual review of cell and developmental biology. 2011; 27:185–211. Epub 2011/08/02.
27. Mader CC, Oser M, Magalhaes MA, Bravo-Cordero JJ, Condeelis J, Koleske AJ, et al. An EGFR-Src-Arg-cortactin pathway mediates functional maturation of invadopodia and breast cancer cell invasion. Cancer research. 2011; 71(5):1730–41. Epub 2011/01/25. [PubMed: 21257711]
28. Oser M, Mader CC, Gil-Henn H, Magalhaes M, Bravo-Cordero JJ, Koleske AJ, et al. Specific tyrosine phosphorylation sites on cortactin regulate Nck1-dependent actin polymerization in invadopodia. Journal of cell science. 2010; 123(Pt 21):3662–73. Epub 2010/10/26. [PubMed: 20971703]
29. Seals DF, Azucena EF Jr, Pass I, Tesfay L, Gordon R, Woodrow M, et al. The adaptor protein Tks5/Fish is required for podosome formation and function, and for the protease-driven invasion of cancer cells. Cancer cell. 2005; 7(2):155–65. Epub 2005/02/16. [PubMed: 15710328]
30. Bowden ET, Barth M, Thomas D, Glazer RI, Mueller SC. An invasion-related complex of cortactin, paxillin and PKCmu associates with invadopodia at sites of extracellular matrix degradation. Oncogene. 1999; 18(31):4440–9. Epub 1999/08/12. [PubMed: 10442635]
31. Clark ES, Whigham AS, Yarbrough WG, Weaver AM. Cortactin is an essential regulator of matrix metalloproteinase secretion and extracellular matrix degradation in invadopodia. Cancer research. 2007; 67(9):4227–35. Epub 2007/05/08. [PubMed: 17483334]
32. Magalhaes MA, Larson DR, Mader CC, Bravo-Cordero JJ, Gil-Henn H, Oser M, et al. Cortactin phosphorylation regulates cell invasion through a pH-dependent pathway. The Journal of cell biology. 2011; 195(5):903–20. Epub 2011/11/23. [PubMed: 22105349]
33. Beaty BT, Sharma VP, Bravo-Cordero JJ, Simpson MA, Eddy RJ, Koleske AJ, et al. beta1 integrin regulates Arg to promote invadopodial maturation and matrix degradation. Molecular biology of the cell. 2013 Epub 2013/04/05.
34. Bravo-Cordero JJ, Marrero-Diaz R, Megias D, Genis L, Garcia-Grande A, Garcia MA, et al. MT1-MMP proinvasive activity is regulated by a novel Rab8-dependent exocytic pathway. The EMBO journal. 2007; 26(6):1499–510. Epub 2007/03/03. [PubMed: 17332756]

35. Liu H, Patel MR, Prescher JA, Patsialou A, Qian D, Lin J, et al. Cancer stem cells from human breast tumors are involved in spontaneous metastases in orthotopic mouse models. Proceedings of the National Academy of Sciences of the United States of America. 2010; 107(42):18115–20. Epub 2010/10/06. [PubMed: 20921380]
36. Sakurai-Yageta M, Recchi C, Le Dez G, Sibarita JB, Daviet L, Camonis J, et al. The interaction of IQGAP1 with the exocyst complex is required for tumor cell invasion downstream of Cdc42 and RhoA. The Journal of cell biology. 2008; 181(6):985–98. Epub 2008/06/11. [PubMed: 18541705]
37. Bravo-Cordero JJ, Oser M, Chen X, Eddy R, Hodgson L, Condeelis J. A novel spatiotemporal RhoC activation pathway locally regulates cofilin activity at invadopodia. Current biology : CB. 2011; 21(8):635–44. Epub 2011/04/09. [PubMed: 21474314]
38. Lessey EC, Guilluy C, Burridge K. From mechanical force to RhoA activation. Biochemistry. 2012; 51(38):7420–32. Epub 2012/08/31. [PubMed: 22931484]
39. Pertz O, Hodgson L, Klemke RL, Hahn KM. Spatiotemporal dynamics of RhoA activity in migrating cells. Nature. 2006; 440(7087):1069–72. Epub 2006/03/21. [PubMed: 16547516]
40. Blouw B, Seals DF, Pass I, Diaz B, Courtneidge SA. A role for the podosome/invadopodia scaffold protein Tks5 in tumor growth in vivo. European journal of cell biology. 2008; 87(8–9):555–67. Epub 2008/04/18. [PubMed: 18417249]
41. Lovett DH, Cheng S, Cape L, Pollock AS, Mertens PR. YB-1 alters MT1-MMP trafficking and stimulates MCF-7 breast tumor invasion and metastasis. Biochemical and biophysical research communications. 2010; 398(3):482–8. Epub 2010/07/06. [PubMed: 20599698]
42. Gil-Henn H, Patsialou A, Wang Y, Warren MS, Condeelis JS, Koleske AJ. Arg/Abl2 promotes invasion and attenuates proliferation of breast cancer in vivo. Oncogene. 2012 Epub 2012/07/11.
43. Hu Y, Kiely JM, Szente BE, Rosenzweig A, Gimbrone MA Jr. E-selectin-dependent signaling via the mitogen-activated protein kinase pathway in vascular endothelial cells. J Immunol. 2000; 165(4):2142–8. Epub 2000/08/05. [PubMed: 10925300]
44. Hu Y, Szente B, Kiely JM, Gimbrone MA Jr. Molecular events in transmembrane signaling via E-selectin. SHP2 association, adaptor protein complex formation and ERK1/2 activation. The Journal of biological chemistry. 2001; 276(51):48549–53. Epub 2001/10/17. [PubMed: 11602579]
45. Laferriere J, Houle F, Taher MM, Valerie K, Huot J. Transendothelial migration of colon carcinoma cells requires expression of E-selectin by endothelial cells and activation of stress-activated protein kinase-2 (SAPK2/p38) in the tumor cells. The Journal of biological chemistry. 2001; 276(36):33762–72. Epub 2001/07/13. [PubMed: 11448946]
46. Rousseau S, Houle F, Landry J, Huot J. p38 MAP kinase activation by vascular endothelial growth factor mediates actin reorganization and cell migration in human endothelial cells. Oncogene. 1997; 15(18):2169–77. Epub 1997/12/11. [PubMed: 9393975]
47. Walz G, Aruffo A, Kolanus W, Bevilacqua M, Seed B. Recognition by ELAM-1 of the sialyl-Lex determinant on myeloid and tumor cells. Science. 1990; 250(4984):1132–5. Epub 1990/11/23. [PubMed: 1701275]
48. Weiss TW, Mehrabi MR, Kaun C, Zorn G, Kastl SP, Speidl WS, et al. Prostaglandin E1 induces vascular endothelial growth factor-1 in human adult cardiac myocytes but not in human adult cardiac fibroblasts via a cAMP-dependent mechanism. Journal of molecular and cellular cardiology. 2004; 36(4):539–46. Epub 2004/04/15. [PubMed: 15081313]
49. Yoshida M, Takano Y, Sasaoka T, Izumi T, Kimura A. E-selectin polymorphism associated with myocardial infarction causes enhanced leukocyte-endothelial interactions under flow conditions. Arteriosclerosis, thrombosis, and vascular biology. 2003; 23(5):783–8. Epub 2003/03/22.
50. Li B, Zhao WD, Tan ZM, Fang WG, Zhu L, Chen YH. Involvement of Rho/ROCK signalling in small cell lung cancer migration through human brain microvascular endothelial cells. FEBS letters. 2006; 580(17):4252–60. Epub 2006/07/11. [PubMed: 16828752]
51. McGhee EJ, Morton JP, Von Kriegsheim A, Schwarz JP, Karim SA, Carragher NO, et al. FLIM-FRET imaging in vivo reveals 3D-environment spatially regulates RhoGTPase activity during cancer cell invasion. Small GTPases. 2011; 2(4):239–44. Epub 2011/12/07. [PubMed: 22145098]
52. Timpson P, McGhee EJ, Morton JP, von Kriegsheim A, Schwarz JP, Karim SA, et al. Spatial regulation of RhoA activity during pancreatic cancer cell invasion driven by mutant p53. Cancer research. 2011; 71(3):747–57. Epub 2011/01/27. [PubMed: 21266354]

53. Carmona-Fontaine C, Matthews HK, Kuriyama S, Moreno M, Dunn GA, Parsons M, et al. Contact inhibition of locomotion in vivo controls neural crest directional migration. Nature. 2008; 456(7224):957–61. Epub 2008/12/17. [PubMed: 19078960]

54. Ponik SM, Trier SM, Wozniak MA, Eliceiri KW, Keely PJ. RhoA is down-regulated at cell-cell contacts via p190RhoGAP-B in response to tensional homeostasis. Molecular biology of the cell. 2013 Epub 2013/04/05.

55. Witzel S, Zimyanin V, Carreira-Barbosa F, Tada M, Heisenberg CP. Wnt11 controls cell contact persistence by local accumulation of Frizzled 7 at the plasma membrane. The Journal of cell biology. 2006; 175(5):791–802. Epub 2006/11/30. [PubMed: 17130287]

56. Arthur WT, Noren NK, Burridge K. Regulation of Rho family GTPases by cell-cell and cell-matrix adhesion. Biological research. 2002; 35(2):239–46. Epub 2002/11/06. [PubMed: 12415742]

57. Nethe M, de Kreuk BJ, Tauriello DV, Anthony EC, Snoek B, Stumpel T, et al. Rac1 acts in conjunction with Nedd4 and dishevelled-1 to promote maturation of cell-cell contacts. Journal of cell science. 2012; 125(Pt 14):3430–42. Epub 2012/04/03. [PubMed: 22467858]

58. Omelchenko T, Hall A. Myosin-IXA regulates collective epithelial cell migration by targeting RhoGAP activity to cell-cell junctions. Current biology : CB. 2012; 22(4):278–88. Epub 2012/02/07. [PubMed: 22305756]

59. Sharma VP, DesMarais V, Sumners C, Shaw G, Narang A. Immunostaining evidence for PI(4,5)P2 localization at the leading edge of chemoattractant-stimulated HL-60 cells. Journal of leukocyte biology. 2008; 84(2):440–7. Epub 2008/05/15. [PubMed: 18477691]

60. Sharma VP, Entenberg D, Condeelis J. High-resolution live-cell imaging and time-lapse microscopy of invadopodium dynamics and tracking analysis. Methods Mol Biol. 2013

61. Lipschutz, JH.; O'Brien, LE.; Altschuler, Y.; Avrahami, D.; Nguyen, Y.; Tang, K., et al. Analysis of membrane traffic in polarized epithelial cells. In: Bonifacino, Juan S., et al., editors. Current protocols in cell biology/editorial board. Vol. Chapter 15. 2001. p. 5Epub 2008/01/30

62. Spiering D, Hodgson L. Multiplex imaging of Rho family GTPase activities in living cells. Methods Mol Biol. 2012; 827:215–34. Epub 2011/12/07. [PubMed: 22144278]

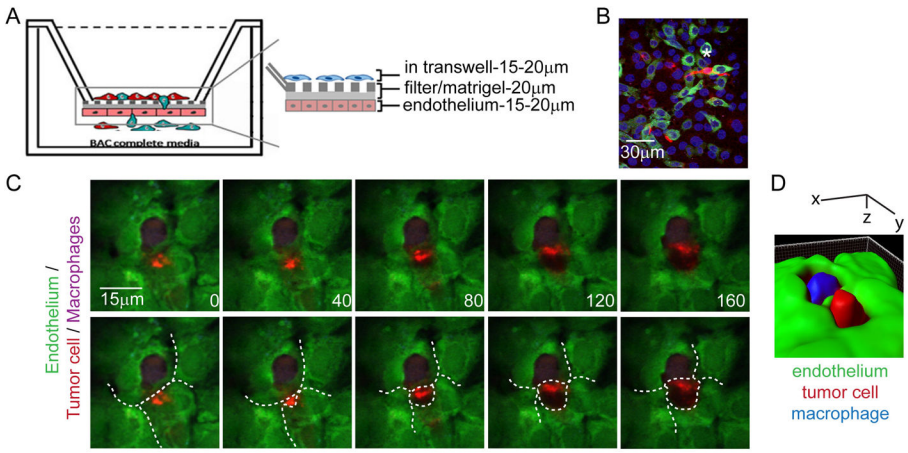

Figure 1.

Tumor cells physically interact with macrophages during transendothelial migration. (A) Diagram of transwell experiment. (B) Fixed image of apical section of transwell with tumor cell (MDA-MB-231-GFP, green) and macrophage (CMPTX-labeled, red) physically interacting in the endothelium (blue, DAPI). Asterisk marks tumor cells in contact with macrophages at endothelium. (C) Still images from en face view of movie of tumor cell (red) transmigrating through endothelium (green) next to a macrophage (purple). Images are every 40 minutes. Dark region of tumor cell is nucleus since dtomato space fill was used. White dashed lines mark edges of endothelial cells (bottom panel). Transendothelial migration of tumor cell is depicted by the broadening of outlined area within the endothelium. (D) IMARIS 3D reconstruction of cells shown in “C” revealing tumor cell (red) penetrating through endothelium (green) in the Z-axis next to a macrophage (blue).

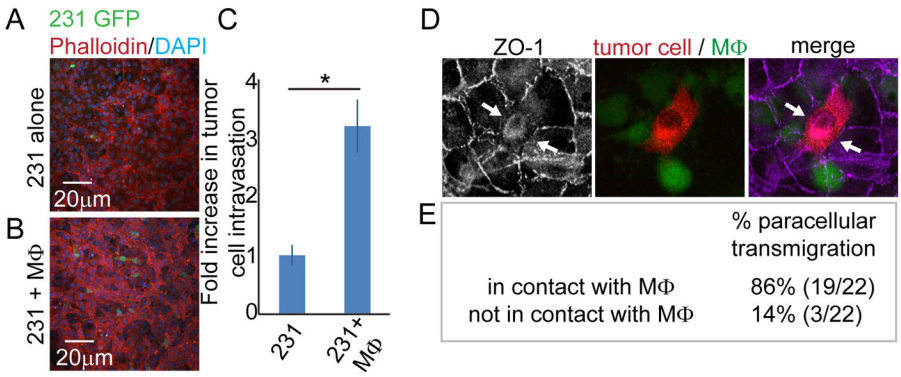

Figure 2.

Macrophages facilitate 231 transendothelial migration. (A) Merge of apical 12 microns of HUVEC transwells. MDA-MB-231 cells alone (green) and endothelium marked by phalloidin-rhodamine (red). (B) Merge of apical 12 microns of HUVEC transwells with MDA-MB-231 cells (green) and macrophages (unlabeled) added. Endothelium marked by phalloidin-rhodamine (red). (C) Quantification of number of MDA-MB-231 cells exposed to the apical surface of HUVEC transwells per field of view (512×512 μm), as a relative number to 231 GFP control. Mean ± SEM, T-test $p<0.05$. n=25 for each, 6 independent experiments. (D) Tight juntions (ZO-1, white) immunostaining of transwells when tumor cell (231 tomato, red) is undergoing transendothelial migration when in contact with a macrophage (green). White arrows mark absence of ZO-1 immunostaining. (E) Quantification of tumor cells undergoing transmigration on transwells when in contact or not in contact with macrophages. n=22, 5 independent experiments.

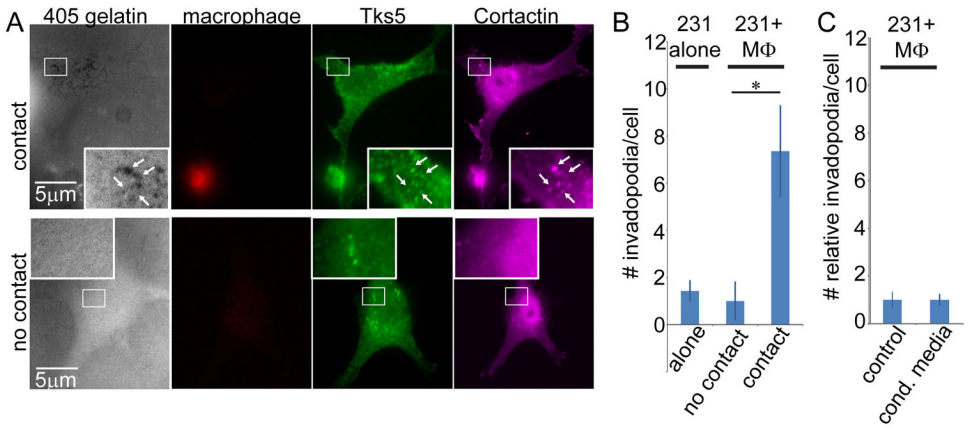

Figure 3.

Macrophages induce invadopodium formation in MDA-MB-231 cells. (A, B) Immunostaining of MDA-MB-231 cells for tks5 and cortactin in the presence and absence of macrophages on 405-labelled gelatin matrix. Top panels shows MDA-MB-231 cell in contact with macrophage (red). Inset is zoomed region of white box in panels. Arrows mark invadopodia, defined as cortactin and tks5 positive invadopodia that degrade matrix. Bottom panels show MDA-MB-231 cell that is not in contact with a macrophage. (B) Quantification of number of invadopodia per cell when MDA-MB-231 cells plated with macrophages or when MDA-MB-231 cells plated alone. Mean ± SEM, ANOVA p = 0.0003. n=60 (alone), 18 (no contact), 41 (contact) cells; 6 independent experiments. (C) Quantification of number of invadopodia per cell when MDA-MB-231 cells plated in BAC1.2F5 conditioned media. Mean ± SEM as a ratio of control. n=34 (ctrl), 30 (conditioned) cells; 2 independent experiments.

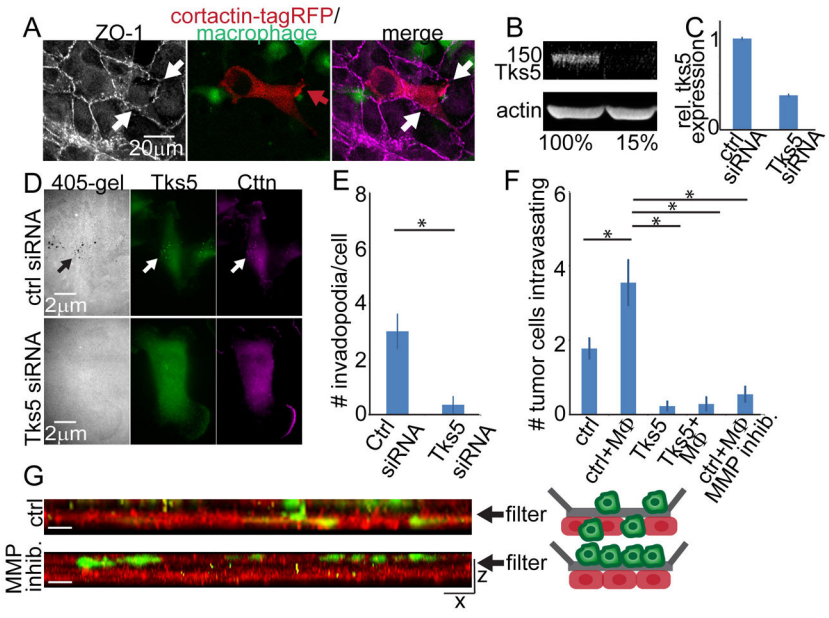

Figure 4.

Invadopodia are required for transendothelial migration. (A) Invadopodia form as MDA-MB-231 cells undergo transendothelial migration. Immunostaining for ZO-1 (white in left panel, purple in merge) of transwells with MDA-MB-231 cells transfected with Cortactin-tagRFP (red). White arrowheads mark lacdisassembled tight junctions. Red arrow marks cortactin enrichment in tumor cell as the cell penetrates through the endothelium. (B) tks5 smartpool siRNA knockdown western blot with actin as loading control. Quantification of tks5 fluorescence below. (C) qRT-PCR of control and Tks5 siRNA cells to show tks5 mRNA reduction in Tks5 siRNA cells. n=3 replicates. (D) Representative images of control and tks5 siRNA MDA-MB-231 cells immunostained for tks5 (green) and cortactin (purple) and matrix degradation (black clearings). Arrows mark invadopodia. (E) Quantification of invadopodia number per cell in control and tks5 siRNA MDA-MB-231 cells plated in complete media. Mean ± SEM, T-test $p<0.05$. n=15 (ctrl), 27 (tks5) cells; 3 independent experiments. (F) Quantification of macrophage-induced in vitro intravasation when MDA-MB-231 cells treated with control siRNA, tks5 siRNA and GM6001 with and without macropahges. Mean ± SEM. n=10 (ctrl), 15 (ctrl+MΦ), 14 (Tks5), 14 (Tks5+MΦ), 11 (MMP inhib); 2 independent experiments for each. ANOVA p=1.4E-11. (G) Representative images of MDA-MB-231 treated with GM6001 for transendothelial cell crossing. X- views of transwells showing tumor cells (green) and endothelium (red), with cartoon depiction to the right. Dark clearing is filter (arrow).

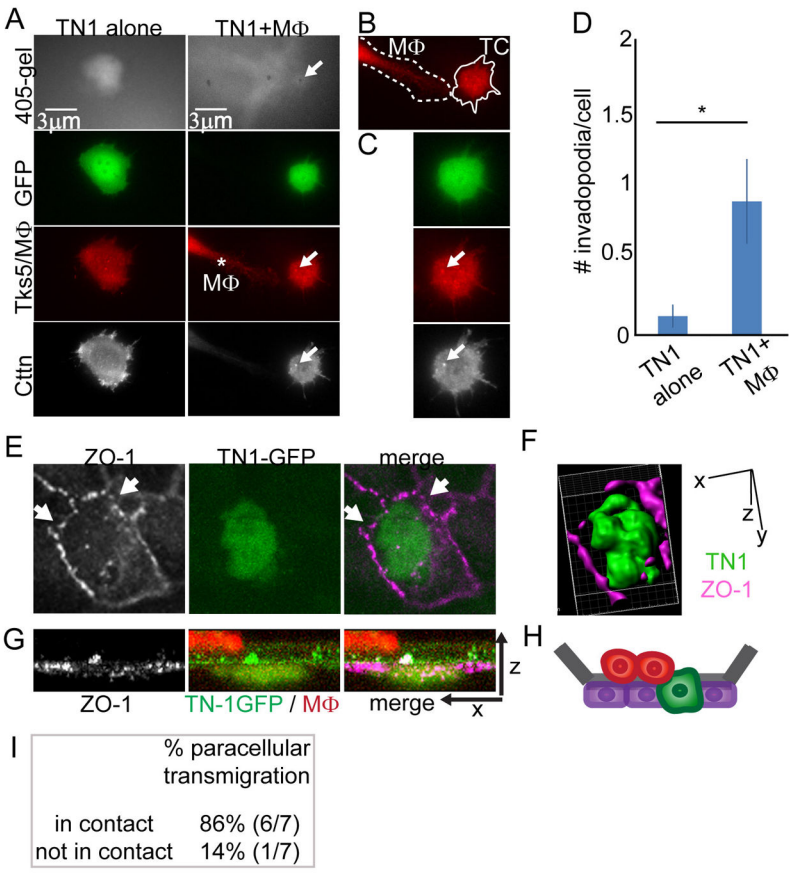

Figure 5.

Patient-derived breast tumor cells form invadopodia and contact macrophages during transendothelial migration. (A) TN1-GFP cells plated with and without macrophages (red) on 405-labelled gelatin coated dishes and immunostained with tks5 (red) and cortactin (white). Macrophage is labeled with CMPTX (red) and is marked by asterisk. Arrow marks invadopodium in TN1 cell in contact with macrophage. (B) As both the macrophage and tks5 immunostaining are in the same channel, GFP is used to specifically detect tumor cells (TN1-GFP). A dashed line outlines the macrophage (MΦ) and a solid line outlines the tumor cell (TC). (C) Zoomed image of tumor cell in (A) to reveal invadopodium (tks5 and cttn-positive) in TN1-GFP tumor cell (arrow). (D) Quantification of macrophage-induced invadodopdia in TN1-GFP cells. n=24 (Tn1 alone), 10 (TN1+MΦ) cells; 2 independent experiments. T-test $p<0.05$. (E) TN1-GFP cells plated on transendothelial migration transwells. Arrows marks areas of ZO-1 disassembly (white in left panel, purple in merge). (F) IMARIS 3D reconstruction of TN1 cell in (E) to show TN1-GFP (green) cell in z-axis penetrating through endothelium, as tight junctions (pink) are disassembling. (G) Z projection of same TN-1-GFP cell in (E) undergoing transendothelial migration (endothelium marked by white ZO-1 immunostaining in left panel, purple ZO-1 in merge in right panel) when contacting macrophages (red). (H) Cartoon depiction of macrophage-induced TN1-GFP transmigration in (G). (I) Quantification of TN1-GFP cells undergoing in vitro intravasation when in contact and not in contact with macrophages. n=7; 2 independent experiments.

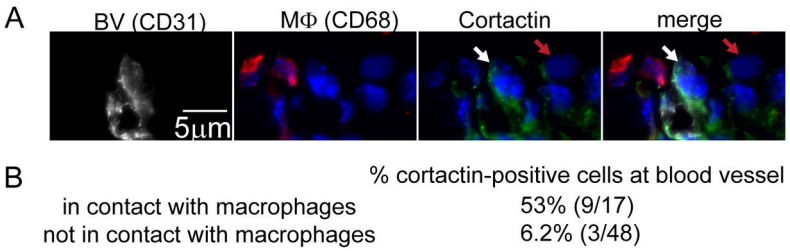

Figure 6.

Physical contact between macrophages and tumor cells at blood vessels correlates with increased invadopodium formation in vivo. (A) Immunostained sections from MDA-MB-231 orthotopic tumor. Cortactin (green) is enriched in tumor cell (cells indicated by DAPI, blue) in contact with macrophage (CD68, red) at blood vessel (CD31, white). White arrow marks tumor cell with increased cortactin intensity when in contact with macrophage. Red arrow marks tumor cell with absent cortactin immunostaining when not in contact with macrophage. (B) Quantification of % cortactin-positive cells at blood vessel when in contact and not in contact with macrophages. n=6 sections from 3 tumors.

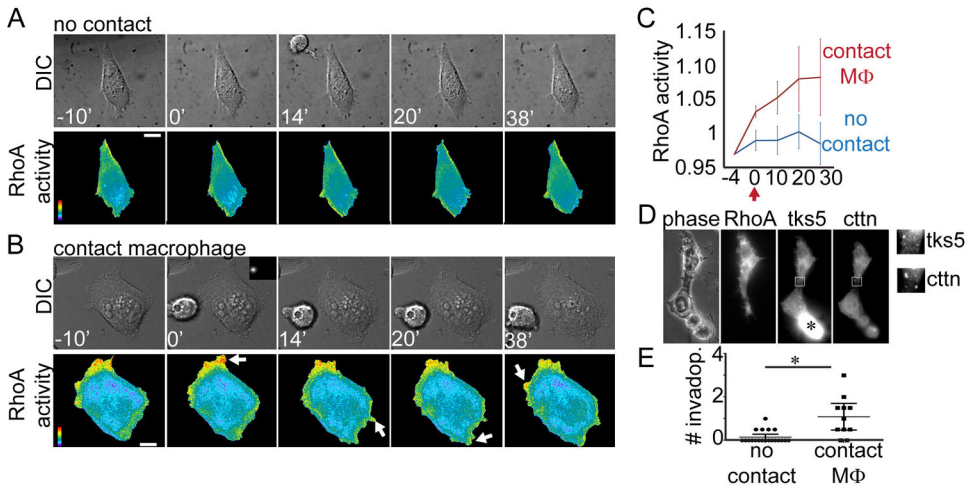

Figure 7.

Macrophages induce RhoA signaling in tumor cells to form invadopodia. (A) RhoA biosensor expressing MDA-MB-231 cell not in contact with macrophages. DIC panels (top) and FRET panels (bottom) reveal no global increase in RhoA activity nor protrusive structures. Time interval is indicated in minutes relative to macrophage addition. DIC panel corresponding to time 0 contains inset of TRITC to show absence of cell tracker red labeled macrophage. (B) RhoA biosensor expressing cell in contact with macrophage. DIC panels (top) reveals close association of macrophage and tumor cell. DIC panel corresponding to time 0 contains inset of TRITC to reveal cell tracker red labeled macrophage. FRET panels (bottom) show increased RhoA activity upon macrophage contact as well as multiple protrusions (white arrows). Time interval is indicated in minutes relative to macrophage addition. The pseudocolored scale in (A) and (B) represents ratio limits of black (1.0) to red (1.5) for RhoA activity. Scale bar is 10μm. (C) Quantification of RhoA biosensor activity in cells contacting macrophages (red) compared to cells not contacting macrophages (blue). Plotted is Mean ± SEM. Red arrow marks time in minutes when macrophages are added. n=12 (contact), 15 cells (no contact); 3 independent experiments. (D) RhoA biosensor expressing cells were imaged for 1 hour, and subsequently fixed and immunostained for cortactin and tks5. Asterisk in tks5 panel marks macrophage. Boxed area in images are shown on right to reveal punctae that are both tks5 and cortactin positive. (E) Quantification of invadopodium formation (tks5 and cortactin-positive structures) in RhoA biosensor-expressing cells that contact macrophages versus cells that do not contact macrophages. Plotted are all values, as well as mean ± SEM, T-test $p<0.05$. n=20 (no contact), 11 (contact); 2 independent experiments.